

This article was downloaded by:

On: 25 January 2011

Access details: *Access Details: Free Access*

Publisher *Taylor & Francis*

Informa Ltd Registered in England and Wales Registered Number: 1072954 Registered office: Mortimer House, 37-41 Mortimer Street, London W1T 3JH, UK



## Liquid Crystals

Publication details, including instructions for authors and subscription information:

<http://www.informaworld.com/smpp/title~content=t713926090>

### Thermal properties of non-symmetric bibenzoate liquid crystalline dimers

Aránzazu Del Campo Corresponding author<sup>a</sup>; Andreas Meyer<sup>b</sup>; Ernesto Pérez<sup>a</sup>; Antonio Bello<sup>a</sup>

<sup>a</sup> Instituto de Ciencia y Tecnología de Polímeros (C.S.I.C.), Juan de la Cierva, 3. 28 006 Madrid, Spain <sup>b</sup> Beamline A2, HASYLAB Notkestrasse, 85. 22 603 Hamburg, Germany

Online publication date: 19 May 2010

**To cite this Article** Campo Corresponding author, Aránzazu Del , Meyer, Andreas , Pérez, Ernesto and Bello, Antonio(2004) 'Thermal properties of non-symmetric bibenzoate liquid crystalline dimers', *Liquid Crystals*, 31: 1, 109 – 118

**To link to this Article:** DOI: 10.1080/0267829032000159105

**URL:** <http://dx.doi.org/10.1080/0267829032000159105>

PLEASE SCROLL DOWN FOR ARTICLE

Full terms and conditions of use: <http://www.informaworld.com/terms-and-conditions-of-access.pdf>

This article may be used for research, teaching and private study purposes. Any substantial or systematic reproduction, re-distribution, re-selling, loan or sub-licensing, systematic supply or distribution in any form to anyone is expressly forbidden.

The publisher does not give any warranty express or implied or make any representation that the contents will be complete or accurate or up to date. The accuracy of any instructions, formulae and drug doses should be independently verified with primary sources. The publisher shall not be liable for any loss, actions, claims, proceedings, demand or costs or damages whatsoever or howsoever caused arising directly or indirectly in connection with or arising out of the use of this material.

# Thermal properties of non-symmetric bibenzoate liquid crystalline dimers

ARÁNZAZU DEL CAMPO\*, ANDREAS MEYER†, ERNESTO PÉREZ and ANTONIO BELLO

Instituto de Ciencia y Tecnología de Polímeros (C.S.I.C.), Juan de la Cierva, 3. 28 006 Madrid, Spain

†Beamline A2, HASYLAB Notkestrasse, 85. 22 603 Hamburg, Germany

(Received 22 April 2002; in final form 14 July 2003; accepted 28 August 2003)

The liquid crystal behaviour of a family of non-symmetric liquid crystalline dimers is reported. These systems contain two bibenzoate rigid units that are linked to distinct terminal groups at one end, and to a flexible interconnecting spacer at the other. Several systems having different terminal and central chains are studied using calorimetric, microscopic and diffraction techniques. All the samples form phases with variable degrees of order (from low ordered smectic to crystalline phases) depending on the chemical constitution of the different segments. The influence of the length, parity and lateral substitution of the spacers on the transitional properties and the symmetry of the mesophases that are formed is analysed. It is found that a decrease in the transition temperatures and enthalpies occurs when the length of the flexible spacers increases, when lateral methyl substituents are introduced, or when the parity of the central spacer changes from an even to odd number of carbon atoms or ether groups. The arrangement of the mesogens and dissimilar flexible groups within the ordered structure is discussed with respect to the observed  $L/d$  ratios. Different values were obtained depending on the parity of the central spacer and on the degree of order. Interpenetrated structures, in which the flexible groups of different lengths are mixed, seem to be compatible with low ordered smectic phases, but sterically disfavoured when constructing crystalline phases.

## 1. Introduction

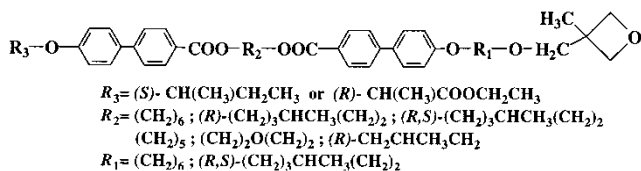
Liquid crystalline symmetric dimers, or twin molecules, are composed of two identical mesogenic groups that have attached at one end a terminal chain of variable length, and at the other an interconnecting flexible spacer [1]. The length, parity, and symmetry of the central spacer have been shown to have an important influence on the thermal properties of the system [2]. The most general manifestation of this *spacer effect* is the alternation in the clearing temperatures and in the enthalpy and entropy changes associated with the phase transitions observed on varying the number of carbon atoms in the spacer [3]. Similar effects have also been observed in main chain liquid crystal polymers (LCPs) and, therefore, LC dimers have been used as model compounds for understanding the properties of the more complex macromolecular systems [4]. In some cases, even the

type of mesophase that is formed on cooling is affected by the nature of the spacer. As an example, certain dimers and main chain LCPs containing bibenzoate units and methylenic or oxymethylenic central spacers show either SmA or SmC<sub>alt</sub> mesophases when the alkyl chain contains an even or odd number of atoms, respectively [5, 6]. The introduction of a methyl substituent in an asymmetric position in even spacers leads to the formation of SmC mesophases [7, 8], or SmC\* phases if only one of the enantiomers is present. These features can be understood by considering the conformational constraint imposed by the spacer: the differences between odd, even or laterally substituted spacers are reflected in differences in the average molecular shape [9].

In the description of the phase behaviour of dimers, the nature of the terminal chains [10], and their ability to be incorporated into the mesophase structure without distorting the packing tendencies dictated by the central spacer, must be also considered. Even more complex are the cases where the terminal groups are not identical, as in non-symmetric dimers. The competition between the differing length scales and dipolar

\*Author for correspondence; Present Address: Max Planck Institut für Polymerforschung, Ackermannweg 10, 55 128 Mainz, Germany; e-mail: delcampo@mpip-mainz.mpg.de

interactions of the different flexible segments in such systems provides an additional source for liquid crystalline polymorphism [3]. In order to enhance our understanding of these effects, this work describes the mesophase behaviour of several non-symmetric dimers containing the biphenyl moiety as the rigid group and a polymerizable oxetane unit at just one end. The chemical structure is,



where  $R_1$ ,  $R_2$  and  $R_3$  are methylenic or oxymethylenic spacers. The names of the different systems are abbreviated as  $\text{Ox}_{R_3}\text{-}R_2\text{-}R_1$ .  $R_3$  is represented by the subscript 1 or 2 depending on whether it is a 2-butyl or a 2-ethylpropionyl group, respectively.  $R_2$  and  $R_1$  are abbreviated by the number of carbon atoms contained in the spacer,  $C_n$ . The final structures and names of the different oxetanes are shown in table 1 (see also the table heading for the equivalences of the notation employed).

Taking into account previous results known for symmetric dimers and main chain LCPs [4, 7], a careful

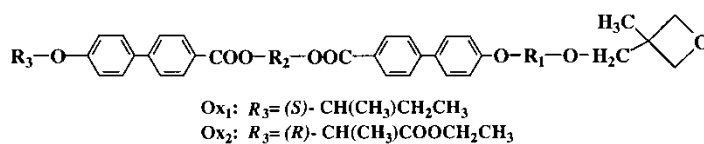
choice of the lengths and nature of the spacers was made. The  $R_3$  terminal group contains an asymmetric centre in order to assist the development of the smectic symmetry and to provide chirality to promote the formation of a  $\text{SmC}^*$  phase. The introduction of the polymerizable oxetane unit at the end of the  $R_1$  group opens the possibility of synthesizing a side chain LCP in a subsequent step, in which the whole dimer structure is attached to a flexible polymeric backbone [11].

The aim of our work is to establish the extent to which the relationships between the structure of the central spacer and properties known for dimers and main chain polymers may be transferred to non-symmetric dimers and the corresponding side chain polymers. In addition, and taking into account the ability of the bibenzoate unit to form  $\text{SmC}^*$  and  $\text{SmCA}$  phases given appropriate flexible spacers, these polymerizable dimers open the possibility to obtain new ferroelectric and antiferroelectric systems for application in electro-optical devices [12].

## 2. Experimental

Differential scanning calorimetry measurements were carried out using a Perkin Elmer DSC7 calorimeter connected to a cooling system. Different scanning rates (20, 10 or  $5^\circ\text{C min}^{-1}$ ) were used. The liquid crystalline textures were observed with a Karl Zeiss polarizing

Table 1. Transition temperatures and enthalpies of the non-symmetric dimers obtained from DSC measurements performed at a heating of  $10^\circ\text{C min}^{-1}$ . Data correspond to reheat scans. The abbreviations Sm, 3D and I correspond to the low-ordered smectic phase, to the phase with three-dimensional positional order, and to the isotropic phase respectively.  $T_g$  denotes the glass transition temperature.  $\Delta C_p$  is given in  $\text{kJ mol}^{-1} \text{K}^{-1}$ . In the names of the dimers:  $C_5 = (\text{CH}_2)_5$ ;  $C_6 = (\text{CH}_2)_6$ ;  $C_4\text{O} = (\text{CH}_2)_2\text{O}(\text{CH}_2)_2$ ;  $C_6\text{Me} = (\text{CH}_2)_2\text{CH}(\text{CH}_3)(\text{CH}_2)_3$ ;  $C_6\text{Me}^* = (R)\text{-(CH}_2)_2\text{CH}(\text{CH}_3)(\text{CH}_2)_3$ ;  $C_3\text{Me}^* = (R)\text{-CH}(\text{CH}_3)(\text{CH}_2)_2$ .



Dimer	Transition temperatures in $^\circ\text{C}$ ( $\Delta H$ in $\text{kJ mol}^{-1}$ ) [ $\Delta S/R$ ]				
	$T_{\text{I} \rightarrow \text{Sm}}$	$T_{\text{I} \rightarrow 3\text{D}}$	$T_g$ ( $\Delta C_p$ )	$T_{3\text{D} \rightarrow \text{I}}$	$T_{\text{Sm} \rightarrow \text{I}}$
$\text{Ox}_2\text{-}C_5\text{-}C_6$	-1.2 (2.4) [1.1]	—	-17 (0.27)	—	11 (3.4) [1.4]
$\text{Ox}_2\text{-}C_4\text{O}\text{-}C_6$	—	8 (12.2) [5.2]	—	19 (11.8) [4.1]	—
$\text{Ox}_2\text{-}C_6\text{-}C_6$	—	47 (33) [12.5]	—	58.7 (8.4) [3] 68.7 (30.6) [10.7]	—
$\text{Ox}_2\text{-}C_6\text{Me}^*\text{-}C_6$	-0.8 (3.3) [1.5]	—	-15 (0.45)	—	5.3 (3.4) [1.5]
$\text{Ox}_1\text{-}C_6\text{Me}^*\text{-}C_6\text{Me}$	-3.4 (6.2) [2.7]	—	-19 (0.40)	37 <sup>a</sup>	5.6 (6.2) [2.7]
$\text{Ox}_1\text{-}C_6\text{Me}\text{-}C_6\text{Me}$	-3.1 (6.8) [3]	—	-15 (0.35)	46 <sup>a</sup>	11.1 (6.8) [2.9]
$\text{Ox}_1\text{-}C_6\text{Me}\text{-}C_6$	25 (6.2) [2.5]	—	-11 (0.46)	—	32 (6.8) [2.7]
$\text{Ox}_1\text{-}C_3\text{Me}^*\text{-}C_6$	—	80 (21.8) [7.4]	—	85 (22.6) [7.6]	—

<sup>a</sup>Data corresponding to the annealed sample.

optical microscope, equipped with a Linkam TMS 92 hot stage and a LNP cooling system.

X-ray scattering experiments were performed using synchrotron radiation ( $\lambda=0.150$  nm) in the beamline A2 at HASYLAB (Hamburg, Germany). Two linear position-sensitive detectors were used simultaneously, one of them covering the  $2\theta$  range from  $10^\circ$  to  $30^\circ$  approximately (WAXS region), and the other from  $1.1^\circ$  to  $8.8^\circ$  (MAXS region, spacings from 8 to 1 nm). Heating and cooling rates of 2 or  $4^\circ\text{C min}^{-1}$  were employed, acquiring data in time frames of 30 s. Subambient experiments were performed using a cooling device that allows cooling to about  $-16^\circ\text{C}$ .

### 3. Synthesis

A detailed procedure for the synthesis of the oxetanes has been published elsewhere [13]. Briefly, 4-hydroxy-4'-biphenylcarboxylic acid was used as the mesogenic precursor, and the flexible chains  $R_2$  and  $R_3$  at each end were attached by reaction with the corresponding alcohol under Mitsunobu conditions [14]. In the final step, the oxetane ring is introduced in the structure by a Williamson etherification of the phenolic group with 3-[(4-methyl-6-bromohexyloxy)methyl]-3-methyloxetane or 3-(6-bromohexyloxy)methyl-3-methyloxetane in a phase-transfer reaction [15]. Great efforts were made during the purification of the final products (by chromatography and successive recrystallization processes), since the presence of impurities is known strongly to affect the phase behaviour of liquid crystalline compounds. In addition, impurities would also hinder the subsequent cationic ring-opening polymerization of the oxetane ring. According to the agreement between the experimental and theoretical results of the elemental analysis, and to the absence of unexpected signals in the  $^1\text{H}$  NMR spectra (200 MHz Varian Spectrometer) [13], a high degree of purity was obtained in all cases.

### 4. Results and discussion

The thermal behaviour of the oxetanes was studied first by differential scanning calorimetry. The DSC curves recorded at a scanning rate of  $10^\circ\text{C min}^{-1}$  for all the compounds are shown in figure 1. The transition temperatures and the molar transition enthalpies and entropies calculated from the reheat scan are listed in table 1. The systems with  $\text{C}_6\text{Me}$  or  $\text{C}_5$  as the central spacer are viscous oils at room temperature that undergo phase transitions at temperatures below  $10^\circ\text{C}$  and become glassy below  $-10^\circ\text{C}$ .  $\text{Ox}_2\text{-C}_6\text{-C}_6$  and  $\text{Ox}_1\text{-C}_3\text{Me}^*\text{-C}_6$  are solids at ambient temperature and no glass transition is detected in the DSC experiment. A glass transition is also not seen in the sample with  $\text{C}_4\text{O}$

as the central spacer. The absence of a glass transition in these last three samples is an indication of a high degree of order in the phases that are involved.

The second heating curve shows the same profile as the cooling curve but inverted, indicating that the same but reversed phase sequence occurs before melting and, therefore, all the phases are enantiotropic. Only  $\text{Ox}_2\text{-C}_6\text{-C}_6$  shows an additional transformation in the heating curve as a consequence of a cold crystallization process.

The entropy and enthalpy values of the thermal transitions obtained for the dimers with  $\text{C}_6\text{Me}$  and  $\text{C}_5$  as the central  $R_2$  spacer ( $\Delta S/R < 3$  and  $\Delta H < 6$   $\text{kJ mol}^{-1}$ ) fall within the range seen for isotropic $\rightarrow$ low ordered smectic (I $\rightarrow$ Sm) or isotropic $\rightarrow$ nematic (I $\rightarrow$ N) transitions for other non-symmetric dimers published in the

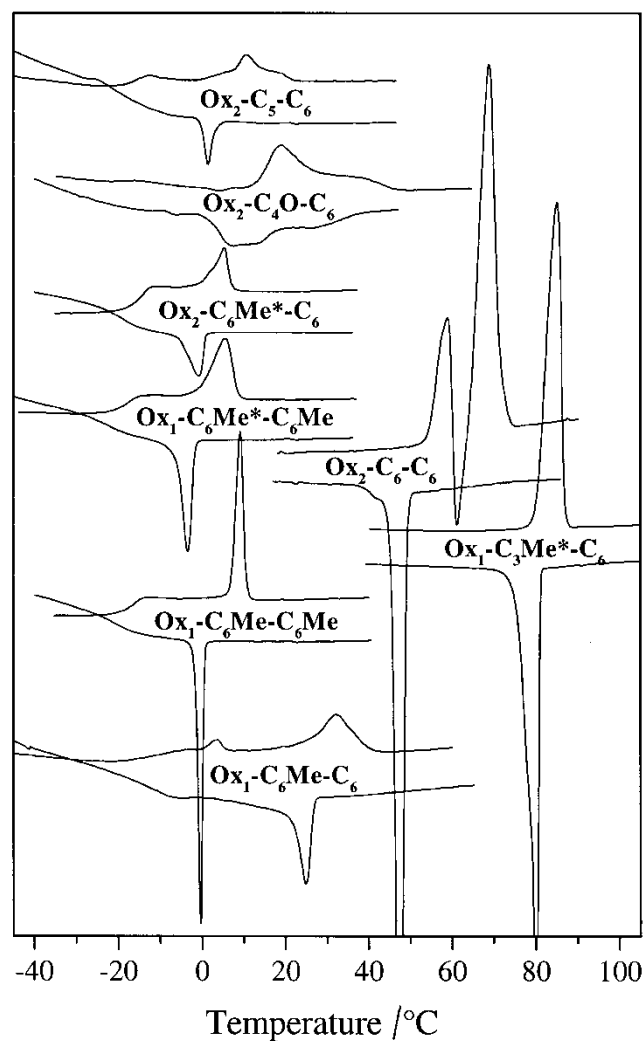


Figure 1. Normalized DSC cooling and reheating curves of the non-symmetric dimers recorded at a scanning rate of  $10^\circ\text{C min}^{-1}$ .

literature ( $\Delta S/R < 3$ , and  $\Delta H \approx 10 \text{ kJ mol}^{-1}$  for smectics or  $\Delta H < 5 \text{ kJ mol}^{-1}$  for nematics) [16, 17]. However, they are smaller than those found for I→Sm transitions of symmetric dimers derived from the bibenzoate unit ( $4 < \Delta S/R < 6$ ,  $14 < \Delta H < 23 \text{ kJ mol}^{-1}$ ) [3]. The endotherms and exotherms shown by  $\text{Ox}_1\text{-C}_6\text{Me-C}_6\text{Me}$ , where  $R_1 = R_2$ , are particularly sharp (width at half-height,  $\Delta w_{1/2} = 1^\circ\text{C}$ ) when compared with the other systems with  $R_2 = \text{C}_6\text{Me}$  but containing a  $R_2 \neq R_1$  ( $\Delta w_{1/2} \approx 4^\circ\text{C}$ ), although the corresponding values for  $\Delta H$  and  $\Delta S$  of the transitions fall in the same range. This result suggests that the similarity in the chemical structure of the flexible spacers  $R_1$  and  $R_2$  facilitates the packing of the dimers in the mesophase. In fact,  $\text{Ox}_1\text{-C}_6\text{Me}^*\text{-C}_6\text{Me}$  shows intermediate behaviour ( $\Delta w_{1/2} = 1.9^\circ\text{C}$ ), in accordance with the similar chemical structure but different stereochemistry of  $R_1$  and  $R_2$ .

$\text{Ox}_2\text{-C}_6\text{-C}_6$  and  $\text{Ox}_1\text{-C}_3\text{Me}^*\text{-C}_6$  show thermal transitions at higher temperatures and with enthalpy and entropy changes that are of the same order of magnitude as those found in asymmetric dimers which exhibit a transition to a crystalline phase [18]. The second endotherm detected on heating  $\text{Ox}_2\text{-C}_6\text{-C}_6$  is very much dependent on both the cooling and the heating rates, as well as on the final temperature of the previous cooling experiment, as usually observed for recrystallization processes, see figure 2. The melting curves after crystallization at  $10^\circ\text{C min}^{-1}$  show different shapes depending on the rate of the reheating experiment. The higher the heating rate, the lower the recrystallization peak, due to the shorter time allowed to the system for the rearrangement. The influence of final temperature in the cooling process explains the differences in the profile of the reheating curves at  $10^\circ\text{C min}^{-1}$  of  $\text{Ox}_2\text{-C}_6\text{-C}_6$  in figure 1 (final cooling temperature was  $-10^\circ\text{C}$ ) and figure 2 (final cooling temperature was  $30^\circ\text{C}$ ). The nature of the phases involved will be discussed later.

With regard to the structure of the non-symmetric

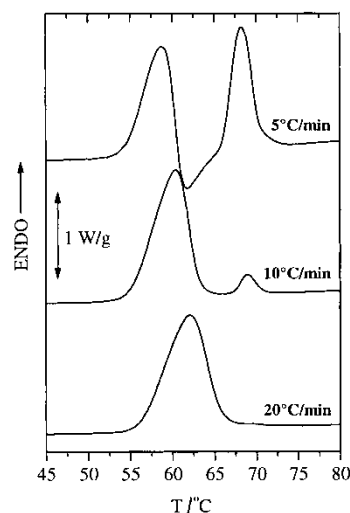


Figure 2. DSC melting curves for  $\text{Ox}_2\text{-C}_6\text{-C}_6$  cooled from the isotropic melt to  $30^\circ\text{C}$  at  $10^\circ\text{C min}^{-1}$  and reheated at three different rates. The curves have been multiplied by the corresponding factors in order to get an apparent normalization in the heat flow data.

dimers and their thermal behaviour, the following trends can be seen:

- Changing the 2-butyl chain  $R_3$  to a slightly longer one, 2-ethylpropionyl, leads to a decrease in the transition temperatures and enthalpies (compare, for example, the thermal data listed in table 1 for  $\text{Ox}_2\text{-C}_6\text{Me}^*\text{-C}_6$  with a longer terminal chain, with those of  $\text{Ox}_1\text{-C}_6\text{Me-C}_6$ ).
- The oxetanes with a central spacer with an even number of carbon atoms or ether units show in general higher values of the temperatures and enthalpies than odd spacers (compare, for example,  $\text{Ox}_2\text{-C}_6\text{-C}_6$  with  $\text{Ox}_2\text{-C}_5\text{-C}_6$  or  $\text{Ox}_2\text{-C}_4\text{O-C}_6$ ). This odd–even alternation of the transition temperatures and enthalpies depending on the parity of the spacer between the mesogens,  $R_2$ , has been found

Table 2. X-ray spacings given in nm of the dimers obtained in real-time synchrotron diffraction experiments.  $L$  represents the calculated length of the structure in an all-*trans*-conformation. The abbreviations Sm and 3D correspond to the low-ordered smectic phase and to the one with three-dimensional positional order respectively.  $\text{C}_5 = (\text{CH}_2)_5$ ;  $\text{C}_6 = (\text{CH}_2)_6$ ;  $\text{C}_4\text{O} = (\text{CH}_2)_2\text{O}(\text{CH}_2)_2$ ;  $\text{C}_6\text{Me} = (\text{CH}_2)_2\text{CH}(\text{CH}_3)(\text{CH}_2)_3$ ;  $\text{C}_6\text{Me}^* = (R)\text{-}(\text{CH}_2)_2\text{CH}(\text{CH}_3)(\text{CH}_2)_3$ ;  $\text{C}_3\text{Me}^* = (R)\text{-CH}(\text{CH}_3)(\text{CH}_2)_2$ .

$\text{Ox}_{R_3}\text{-R}_2\text{-R}_1$	$L$	$d_{\text{Sm}}^{\text{MAXS}}$	$L/d_{\text{Sm}}$	$d_{3\text{D}}^{\text{MAXS}}$	$L/d_{3\text{D}}$	$d_{3\text{D}}^{\text{WAXS}}$
$\text{Ox}_2\text{-C}_4\text{O-C}_6$	4.54	—	—	2.9	1.5	0.450; 0.396; 0.320
$\text{Ox}_2\text{-C}_6\text{-C}_6$	4.69	—	—	4.06; 2.04; 1.34; 3.72 <sup>a</sup>	1.1; 1.3 <sup>a</sup>	0.457; 0.424; 0.372; 0.515 <sup>a</sup> ; 0.382 <sup>a</sup>
$\text{Ox}_2\text{-C}_6\text{Me}^*\text{-C}_6$	4.69	2.02	2.3	—	—	—
$\text{Ox}_1\text{-C}_6\text{Me}^*\text{-C}_6\text{Me}$	4.45	2.16	2.1	3.86; 1.89; 1.27 <sup>b</sup>	1.1	0.480; 0.446; 0.394 <sup>b</sup>
$\text{Ox}_1\text{-C}_6\text{Me-C}_6\text{Me}$	4.45	2.18	2	3.72; 1.91; 1.27 <sup>b</sup>	1.2 <sup>b</sup>	0.467; 0.435; 0.387 <sup>b</sup>
$\text{Ox}_1\text{-C}_3\text{Me}^*\text{-C}_6$	4.08	—	—	2.65	1.5	0.458; 0.406; 0.326

<sup>a</sup>Data corresponding to the recrystallization process.

<sup>b</sup>Data corresponding to the annealed sample.

for all symmetric and non-symmetric dimers published in the literature [3, 16–18].

- (c) The presence of lateral methyl substituents in an asymmetric position, either in the central or terminal chains, reduces the symmetry of the systems and consequently the transition temperatures and enthalpies. See, for example, the values found in the case of the linear spacer  $\text{Ox}_2\text{-C}_6\text{-C}_6$  compared with the substituted  $\text{Ox}_2\text{-C}_6\text{Me}^*\text{-C}_6$ . The same tendency is observed when comparing  $\text{Ox}_1\text{-C}_6\text{Me-C}_6\text{Me}$  and  $\text{Ox}_1\text{-C}_6\text{Me-C}_6$ . This tendency has also been observed in other dimers published in the literature [16].
- (d) In the case of  $\text{Ox}_1\text{-C}_3\text{Me}^*\text{-C}_6$ , the particularly short central spacer may also lead to special packing restrictions and therefore to phases of different symmetry when compared with the rest of the dimers synthesized.

It is worth mentioning at this point that the relationships observed between the transitional properties and the nature of the central spacer in these systems are similar to those found in symmetric dimers and main chain liquid crystalline polymers containing similar units [3, 4, 7].

Further analysis of the symmetry of the mesophases was performed with real time X-ray diffraction using synchrotron radiation. The subambient transition temperatures constitute a significant experimental difficulty, so that only selected samples could be analysed. The results are shown in table 2. The X-ray experiments were performed with heating and cooling ramps at a predefined rate. A clear change in the diffraction pattern of the analysed samples could be observed at the same temperatures at which the endotherms and exotherms were detected in the calorimetric experiments. All these phases showed at least one sharp MAXS reflection, characteristic of structures with a layer periodicity, as in smectic mesophases or crystalline phases. Therefore, the formation of nematic phases can be rejected. Different patterns were observed in the WAXS region and these will be described in the following paragraphs.

The diffraction patterns of the oxetanes  $\text{Ox}_2\text{-C}_4\text{O-C}_6$ ,  $\text{Ox}_2\text{-C}_6\text{-C}_6$  and  $\text{Ox}_1\text{-C}_3\text{Me}^*\text{-C}_6$  recorded at room temperature contained at least one sharp MAXS and three sharp WAXS diffraction peaks, corresponding to the formation of crystalline phases with long range three-dimensional positional order. These results are consistent with the calorimetric analysis. As an example, figure 3 shows the diffraction pattern of  $\text{Ox}_2\text{-C}_6\text{-C}_6$  taken at different temperatures during a heating cycle after controlled crystallization at  $4^\circ\text{C min}^{-1}$ . At  $30^\circ\text{C}$  the crystalline phase can be seen, characterized by

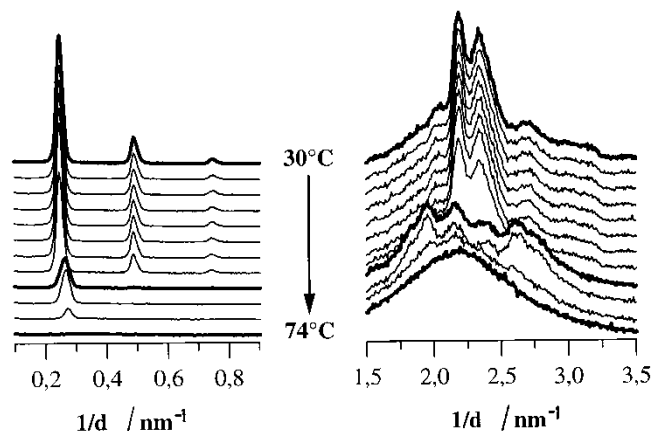


Figure 3. Variable temperature diffraction patterns of  $\text{Ox}_2\text{-C}_6\text{-C}_6$  in the middle and wide angle regions during a heating cycle after crystallization from the melt. The diffractograms in bold lines correspond to those taken at temperatures of  $30^\circ\text{C}$ ,  $62^\circ\text{C}$ , and  $74^\circ\text{C}$  starting from the one at the top. Heating rate is  $4^\circ\text{C min}^{-1}$ .

several WAXS spacings and MAXS first, second and third order reflections. When the temperature approaches  $62^\circ\text{C}$ , these reflections disappear, and new but less well defined reflections are formed, indicating the development of a different crystalline phase (in accordance with the recrystallization process observed in the calorimetric results). The presence of different WAXS reflections and the rather high values of the enthalpies involved in the process are consistent with a Cr–Cr transition and not with the formation of a Sm phase prior to isotropization. Finally, these reflections disappear when heated above  $74^\circ\text{C}$ , leaving the amorphous halo in the WAXS region and no sharp peaks in the MAXS region that corresponds to the isotropic melt. Attempts to obtain mechanically aligned samples were made in order to obtain X-ray data from oriented samples for a detailed analysis of the crystalline lattice. Unfortunately all attempts failed and, in consequence, no unambiguous assignment of the type of crystal is possible.

The X-ray pattern of the dimer  $\text{Ox}_2\text{-C}_4\text{O-C}_6$  performed after cooling from the melt shows the formation of only one crystalline phase, according to the several sharp diffractions detected in the WAXS region. This result is rather surprising, since the shapes of the endotherm and exotherm detected in the DSC experiments suggest the presence of more than one transition. To clarify this point, an analysis of the location of the diffraction peaks and the evolution of the total area with temperature was performed, since these parameters could be more sensitive than the overall profile of the X-ray spectrum to the coexistence of two or more phases. The results of this analysis are shown in

figure 4. The location of the MAXS peak, as well as its total area, does show important changes during the transition (see lower part of figure 4) in such a way that two different regions are observed (in agreement with the DSC results, see upper part of figure 4) yielding different temperature coefficients and area changes. Smectic systems are known to show a high degree of polymorphism, and small molecular rearrangements involving small enthalpy and symmetry changes are often found in their cooling and heating cycles. In the case of molecules with a bent shape, such as  $Ox_2-C_4O-C_6$  due to the presence of an odd central spacer, this polymorphism is even more frequent and may be more complex due to the appearance of polar phases [19, 20]. These phases are often detected and identified by means of the texture changes at the phase transition when observed under the microscope, or by their optical response to electrical fields. Unfortunately, the birefringent textures obtained could not be identified and the preliminary experiments in surface-stabilized cells were also unsuccessful (no aligned monodomains could be obtained and no electro-optic response could be measured). Additional experimental evidence is needed to clarify the origin of the complex DSC profile.

The compounds where  $R_2$  is  $C_6Me$  or  $C_6Me^*$  show

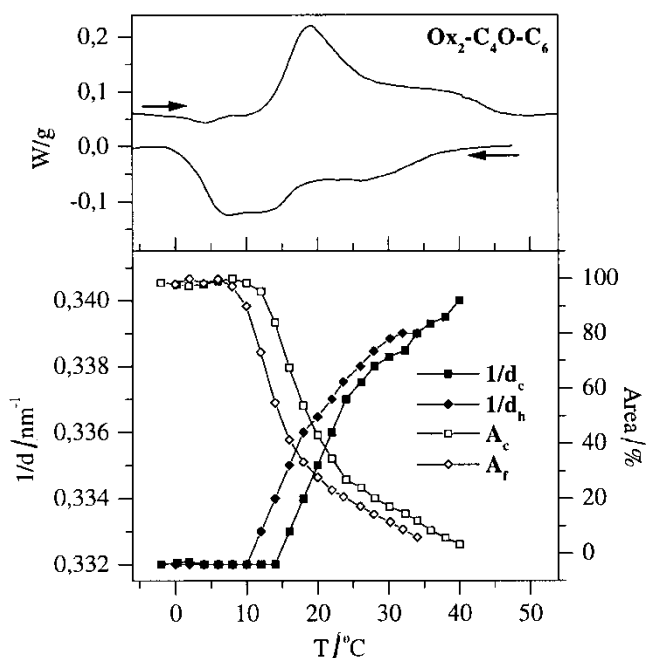


Figure 4. Results of the DSC and real-time diffraction analysis (positions and areas of the MAXS peak) of  $Ox_2-C_4O-C_6$  in a cooling (c) and subsequent heating (h) cycles. The DSC measurements were performed at  $10^\circ C min^{-1}$ . The heating and cooling rates during the X-ray experiment were  $4^\circ C min^{-1}$ . Diffraction diagrams were recorded every  $2^\circ C$ .

the formation of a low ordered mesophase in the cooling and reheating experiments performed at  $4^\circ C min^{-1}$ . The X-ray pattern contains a MAXS diffraction peak, and a broad halo in the WAXS region corresponding to the average lateral distance between the molecules. Figure 5 shows the X-ray analysis during the melting process of  $Ox_1-C_6Me-C_6Me$ . The WAXS halo is centred at 0.45 nm in the mesophase and presents a full width at a half-maximum height of approximately  $0.53 nm^{-1}$ , whereas in the isotropic melt this value increases to  $0.77 nm^{-1}$ . When the sample is left at room temperature for some time, the diffraction pattern of the dimer dramatically changes. Different diffraction peaks appear in the WAXS region (instead of the broad halo) and a new MAXS diffraction peak located at a different spacing is detected, together with its second and third order peaks. These features indicate that the molecules of  $Ox_1-C_6Me-C_6Me$  undergo important rearrangements if they are left for some time above their glass transition, leading to the development of a crystalline phase. In the DSC heating cycle of this new phase only one melting endotherm appears, at  $46^\circ C$ , which means a shift of almost  $40^\circ C$  with respect to the isotropization temperature of the low ordered phase. The calorimetric and diffraction profiles during the heating cycle after annealing are shown in the lower part of figure 5. No trace of the low ordered phase appears in the heating experiment once the more ordered one is completely formed. When the melting temperature is approached, the multiple diffraction peaks gradually loose intensity and disappear to leave the

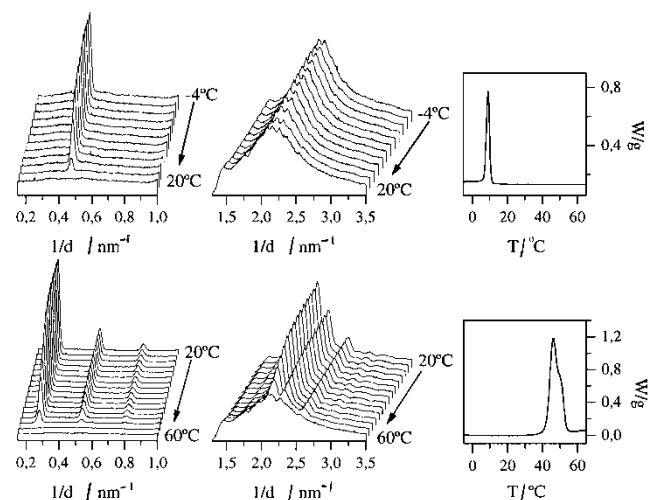


Figure 5. Variable temperature diffraction spectra in the middle and wide angle regions, and the corresponding DSC diagrams, for the heating cycle of  $Ox_1-C_6Me-C_6Me$  after crystallization from the melt at  $20^\circ C min^{-1}$  (top), and after annealing at room temperature for several days (bottom).

characteristic pattern of the isotropic melt. A similar annealing behaviour was found for  $\text{Ox}_1\text{-C}_6\text{Me}^*\text{-C}_6\text{Me}$ .

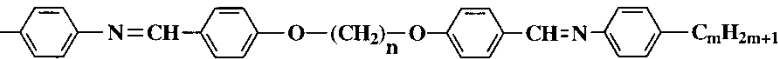
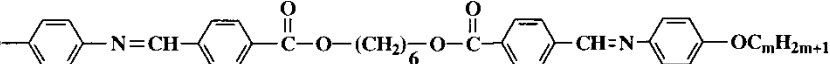
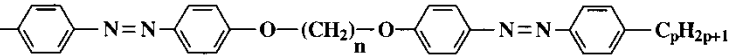
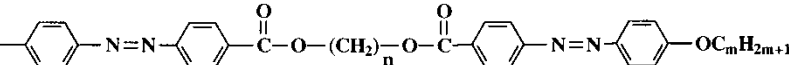
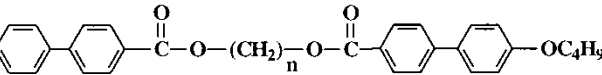
$\text{Ox}_2\text{-C}_6\text{Me}^*\text{-C}_6$ , shows some similarities but also differences in its behaviour with respect to that of the dimers with a comparable central spacer ( $\text{Ox}_1\text{-C}_6\text{Me}^*\text{-C}_6\text{Me}$  and  $\text{Ox}_1\text{-C}_6\text{Me-C}_6\text{Me}$ ). A low ordered smectic phase is also formed in the cooling experiments at temperatures below  $0^\circ\text{C}$ , but no highly ordered structure is obtained when leaving the sample at room temperature, even after several months of annealing.

There are several kinds of low ordered smectic mesophases that are compatible with the X-ray pattern described (orthogonal SmA, tilted SmC or  $\text{SmC}_{\text{alt}}$ ). For differentiation between these phases, either characteristic optical textures or X-ray diffraction experiments with aligned samples are necessary. None of these could be obtained. However, the fact that no considerable change in the MAXS peak position with temperature has been observed experimentally (see upper part of figure 5) seems to be an indication of the formation of orthogonal phases (unless there is an exceptional compensation between a change in the tilt angle and the degree of interpenetration with temperature). This result seems surprising, since symmetric dimers derived from the hydroxybenzoate unit and methylenic central and terminal chains (see last row in table 3) are known to form intercalated SmA mesophases when  $n$  is even,  $\text{SmC}_{\text{alt}}$  phases when  $n$  is odd, and SmC phases if the central spacer has an even number of carbon atoms and

contains a lateral methyl group [21, 22]. Furthermore, main chain liquid crystal polyesters containing analogous structures behave in a similar way [4]. However, changing carboxylic and ether linking groups in these seems to favour the stability range of the orthogonal SmA phase at the expense of the tilted SmC phase [23]. This could be the reason for the absence of SmC phases in the liquid crystalline oxetanes containing a  $\text{C}_6\text{Me}$  central spacer.

Additional information about the specific arrangement of the dimers within the smectic phase is given by the ratio between the calculated length of the molecule in its all-*trans*-conformation and the layer spacing,  $Lld$  [1]. This ratio reflects the degree of interpenetration or segregation of the different flexible groups of the molecule in the LC phase. In general, the formation of smectic phases may be envisioned as a microphase separation in which the mesogenic cores form one region, while the alkyl chains constitute another. There are two major forces responsible for such a separation: energetically, the mean of the core-core and chain-chain interactions is usually more favourable than the mixed core-chain interactions; and entropically, the interaction between a core and a chain acts to order the chain and hence is unfavourable. However, these lateral interactions are not the only factors influencing the microphase separation. Specific electrostatic interactions between polar groups (charge-transfer, quadrupolar interactions) either in the mesogens or in the

Table 3. Structures of different symmetric and non-symmetric dimers and the phases they exhibit.

Dimer	Structure
$\text{H}_{2m+1}\text{C}_m$ - 	Monolayer Sm and N [2]
$\text{H}_{2m+1}\text{C}_m\text{O}$ - 	Monolayer Sm [5]
$\text{H}_{2m+1}\text{C}_m$ - 	Monolayer Sm and N [18]
$\text{H}_{2m+1}\text{C}_m\text{O}$ - 	Intercalated Sm and N [5]
$\text{C}_4\text{H}_9\text{O}$ - 	Intercalated Sm [21]



chains [2, 24], as well as packing or excluded volume factors derived from the differences in length of dissimilar spacers in non-symmetric structures [3, 25, 26] also need to be taken into account. A complex balance of these factors can lead to a segregated bilayer, monolayer or intercalated arrangement of the molecules within the smectic phase, or even to intermediate states between them (interdigitated or interpenetrated phases) [27]. Several examples of dimers from the literature that exhibit the complexity of this interplay are shown in table 3. The formation of one or other structure can be inferred from the  $L/d$  ratio.

The  $L/d$  ratios for the oxetane dimers are given in table 2. In all cases the value of the  $d$ -spacing does not exceed that of the length of the molecule in its all-*trans*-conformation,  $L$ , indicating that there is no tendency to form fully segregated bilayer structures, see figure 6(a). This kind of arrangement is usually found in systems where strong repulsive effects between both ends of the molecule are present. Given the chemical structure of the dimers, the experimental result seems reasonable because no significant unfavourable dipolar interactions between both terminal groups are expected. By contrast, the dependence of the  $L/d$  ratio on the nature of the central spacer is remarkable, suggesting different

arrangements of the mesogens in dimers with even and odd spacers. Thus,  $L/d$  has values close to 1 or 2 for even dimers, but approximately 1.5 in dimers with odd spacers. These results will be discussed in the following paragraphs for each particular case, with reference to the nature of the central spacer and the degree of order present.

The oxetane with a linear even central spacer,  $\text{Ox}_2\text{-C}_6\text{-C}_6$ , has values of  $L/d=1.1$  or  $1.3$  for its two crystalline phases. A value of  $L/d$  close to unity indicates the formation of monolayers. It is assumed that connected mesogens are coparallel, as is known to occur when they are interconnected through an even spacer [9]. A representative picture of the packing of the mesogens is given in figure 6(c). Deviations of the molecule from its all-*trans*-conformation or a low degree of interdigitation of the terminal chains may be responsible for  $L/d$  having values slightly higher than unity, figure 6(d). A monolayer arrangement of the dimer molecules implies that the central and terminal spacers are not mixed within the smectic layers. It is worth mentioning that symmetric dimers with a similar structure reported by Watanabe *et al.* (see last row in table 3) [21] form intercalated SmA and crystalline phases in which the central and terminal chains are

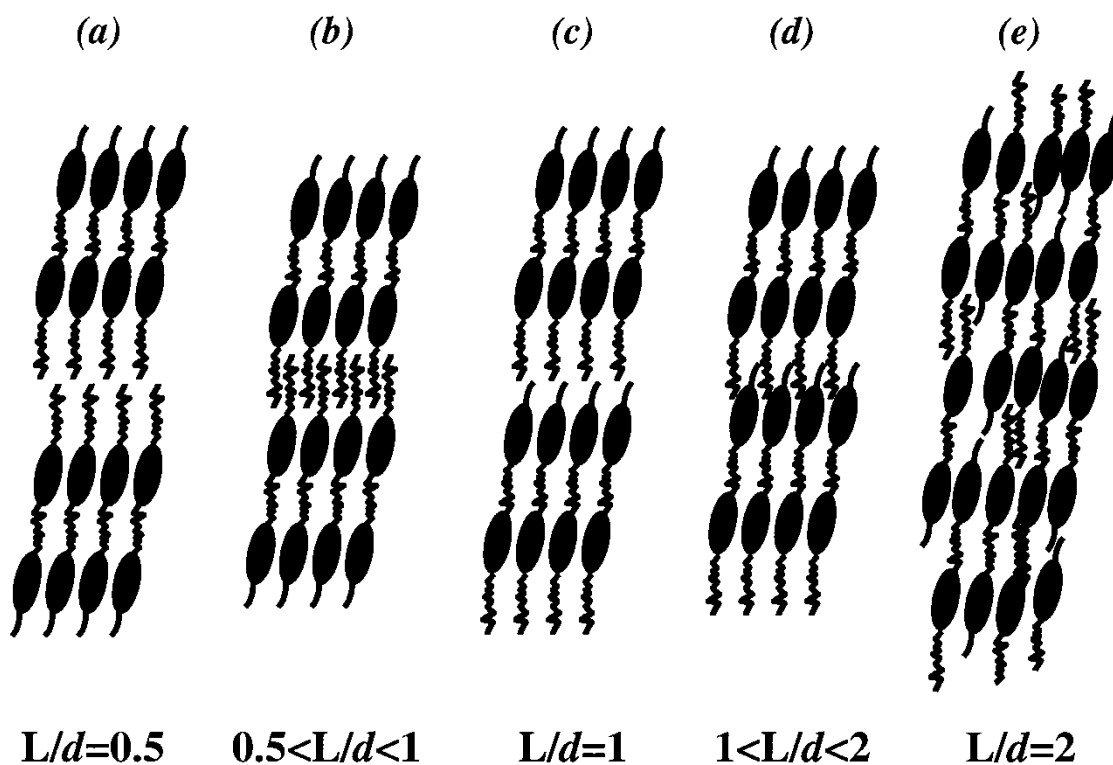


Figure 6. Examples of possible arrangements and the corresponding  $L/d$  ratio of non-symmetric dimers containing an even central spacer. The degree of interpenetration increases from left to right. (a) Bilayer, (b) interdigitated bilayer, (c) monolayer, (d) interdigitated monolayer, (e) intercalated structure.

randomly mixed; see figure 10(c) of [25]. Since in the monolayer and intercalated arrangements, the mesogen–mesogen interactions are the same, this result suggests that the interaction between the terminal chain and the central spacer in the non-symmetric oxetane dimers is unfavourable and destabilizes the intercalated structure. Comparing their chemical structure with the structure of the symmetric dimers of Watanabe [25], the presence of the 3-methyl-oxetane ring seems to be the driving factor for the segregation. The accommodation of the bulky four member ring into an intercalated structure may cost too much energy, with the system preferring to segregate it with in a separated region.

The dimers  $\text{Ox}_1\text{-C}_6\text{Me-C}_6\text{Me}$ ,  $\text{Ox}_1\text{-C}_6\text{Me}^*\text{-C}_6\text{Me}$  and  $\text{Ox}_2\text{-C}_6\text{Me}^*\text{-C}_6$  form a low ordered smectic structure with a value of  $L/d=2\text{--}2.3$  on cooling at  $4^\circ\text{C min}^{-1}$ . This value is consistent with an intercalated structure, see figure 6(e), with a random mixing of the different flexible parts of the dimer in the space between the smectic layers formed by the mesogens. Comparing this result with that obtained for  $\text{Ox}_2\text{-C}_6\text{-C}_6$ , two explanations seem reasonable for the occurrence of intercalation. On one hand, the introduction of a methyl group in the central spacer hinders the close packing of the chains and may leave enough space for the oxetane ring to be accommodated in an intercalated structure [7]. On the other hand, the packing of the molecules in a low ordered smectic is much more fluid than in a crystalline phase and may be compatible with the intercalation of the central spacer and terminal oxetane ring. Space filling constraints may force the flexible chains to arrange separately when the molecules build up a three-dimensional structure. The annealing of  $\text{Ox}_1\text{-C}_6\text{Me-C}_6\text{Me}$  and  $\text{Ox}_1\text{-C}_6\text{Me}^*\text{-C}_6\text{Me}$  leads to the development of a crystalline phase which is now characterized by  $L/d=1.1\text{--}1.2$ , i.e. approaching a monolayer arrangement. The microphase separation in the rapid cooling process seems to be dominated by the unfavourable interaction between aromatic cores and alkyl chains, and therefore intercalated structures are formed in spite of the unfavourable mixing of the terminal group containing the bulky oxetane ring with the linear ones. However, when the sample is allowed to crystallize over a longer time-scale, the system tends to form a more stable crystalline structure in which the terminal oxetane groups are segregated from the central spacers.

The oxetanes containing a central spacer with an odd number of carbon atoms,  $\text{Ox}_2\text{-C}_4\text{O-C}_6$  and  $\text{Ox}_1\text{-C}_3\text{Me}^*\text{-C}_6$ , show a value of  $L/d=1.5$ . This type of molecule is usually bent (as a consequence of the conformational constraints imposed by the central spacer), meaning that connected mesogens arrange in an alternating way

in successive layers. The number of possibilities for the arrangement of these banana-shaped molecules in the layered structure is rather large and, in the case of asymmetric dimers, more complicated structures are also plausible [19, 20]. Therefore, the proposal of an arrangement of the mesogens consistent with  $L/d=1.5$  is not straightforward. Moreover, this evaluation of  $L/d$  assumes that the MAXS diffraction detected experimentally corresponds to the (001) plane, which is not necessarily correct for odd dimers. In alternating phases this diffraction peak may be absent due to symmetry rules. For these reasons, the assignment of an unambiguous structure to the experimental results is not always possible and requires the observation of other experimental data such as an electro-optic response if antiferroelectric phases are formed [28]. Experiments performed in surface-stabilized ferroelectric liquid crystal cells (SSFLCC) showed no response of these systems to an electric field over the whole temperature range. Consequently, an unambiguous description of the position and orientation of the dimers in the smectic structure is not possible at the moment.

## 5. Conclusions

A family of non-symmetric dimers containing bibenzoate units and different central spacers and terminal chains has been characterized. The transitional properties depend on the length and substitution of the flexible spacers in a similar way to symmetric dimers and main chain LCPs. A decrease in the transition temperatures and enthalpies is observed when the length of the flexible spacers increases, when lateral substituents are introduced or when the parity of the central spacer changes from an even to odd number of carbon atoms. Although attractive or repulsive effects due to dipolar interactions between both ends of the molecule are not to be expected, the differences in the length and bulkiness of the spacers seem to introduce some steric incompatibility in the arrangement, disfavoring in some cases the full intercalation of segments and leading to the formation of more stable segregated smectic phases. The results shown here highlight the complex interplay of the different segments in the mesophase formation of liquid crystalline dimers and the need for the synthesis of new compounds in order to be able to establish generalized structure–properties relationships.

The financial support of the *Comisión Interministerial de Ciencia y Tecnología* (Project no. MAT2001-1731) and of the *Fundación Ramón Areces* is gratefully acknowledged. The synchrotron work (in the polymer

line A2 of HASYLAB at DESY, Hamburg) was supported by the IHP Programme 'Access to Research Infrastructures' of the European Commission (Contract HPRI-CT-1999-00040). The authors thank the collaboration of the Hasylab personnel, in particular Drs A. Meyer and S. Funari.

### References

- [1] IMRIE, C. T., and LUCKHURST, G. R., 1998, *Handbook of Liquid Crystals*, Vol. 2B, edited by D. Demus, J. Goodby, G. W. Gray, H. W. Spiess, and V. Vill, (Wiley-VCH), pp. 801–834.
- [2] LUCKHURST, G. R., 1995, *Macromol. Symp.*, **96**, 1; DATE, R. W., IMRIE, C. T., LUCKHURST, G. R., and SEDDON, J. M., 1992, *Liq. Cryst.*, **12**, 203.
- [3] CHOI, S. W., ZENNYOJI, M., TAKANISHI, Y., TAKEZOE, H., NIORI, T., and WATANABE, J., 1999, *Mol. Cryst. liq. Cryst.*, **328**, 185.
- [4] PÉREZ, E., PEREÑA, J. M., BENAVENTE, R., and BELLO, A., 1997, *Handbook of Engineering Polymeric Materials* (New York: Marcel Dekker), pp. 383–397; WATANABE, J., HAYASHI, M., NAKATA, Y., NIORI, T., and TOKITA, M., 1997, *Prog. polym. Sci.*, **22**, 1053.
- [5] NIORI, T., ADACHI, S., and WATANABE, J., 1995, *Liq. Cryst.*, **19**, 139.
- [6] WEISSFLOG, W., RICHTER, S., DIETZMANN, E., RISSE, J., DIELE, S., SCHILLER, P., and PELZL, G., 1997, *Cryst. Res. Technol.*, **32**, 271.
- [7] PÉREZ, E., DEL CAMPO, A., BELLO, A., and BENAVENTE, R., 2000, *Macromolecules*, **33**, 3023; DEL CAMPO, A., PÉREZ, E., BENAVENTE, R., BELLO, A., and PEREÑA, J. M., 1998, *Polymer*, **39**, 3847.
- [8] WATANABE, J., HAYASHI, M., MORITA, A., and TOKITA, M., 1995, *Macromolecules*, **28**, 8073.
- [9] BELLO, A., RIANDE, E., PÉREZ, E., MARUGÁN, M. M., and PEREÑA, J. M., 1993, *Macromolecules*, **26**, 1072; PÉREZ, E., RIANDE, E., BELLO, A., BENAVENTE, R., and PEREÑA, J. M., 1992, *Macromolecules*, **25**, 605; ABE, A., 1984, *Macromolecules*, **17**, 2280.
- [10] OSTROVSKII, B. I., 1993, *Liq. Cryst.*, **14**, 131.
- [11] YUN, Y. K., KO, D. H., JIN, J. I., KANG, Y. S., ZIN, W. C., and JO, B. W., 2000, *Macromolecules*, **33**, 6653; LU, Y. H., and HSU, C. S., 1995, *Macromolecules*, **28**, 1673.
- [12] LAGERWALL, S. T., 1999, *Ferroelectric and Antiferroelectric Liquid Crystals* (Wiley-VCH).
- [13] DEL CAMPO, A., BELLO, A., and PÉREZ, E., 2002, *Macromol. Chem. Phys.*, **203**, 975.
- [14] MITSUNOBU, O., 1981, *Synthesis* 1.
- [15] KAWAKAMI, Y., TAKAHASHI, K., and HIBINO, H., 1991, *Macromolecules*, **24**, 4531.
- [16] BLATCH, A. E., FLETCHER, I. D., and LUCKHURST, G. R., 1997, *J. mater Chem.*, **7**, 9.
- [17] BLATCH, A. E., FLETCHER, I. D., and LUCKHURST, G. R., 1995, *Liq. Cryst.*, **18**, 801.
- [18] BLATCH, A. E., and LUCKHURST, G. R., 2000, *Liq. Cryst.*, **27**, 775.
- [19] ZENNYOJI, M., TAKANISHI, Y., ISHIKAWA, K., THISAYUKTA, J., WATANABE, J., and TAKEZOE, H., 1999, *J. mater. Chem.*, **9**, 2775.
- [20] TUFFIN, R. P., GOODBY, J. W., BENNEMANN, D., HEPPKE, G., LÖTZSCH, D., and SCHEROWSKY, G., 1995, *Mol. Cryst. liq. Cryst.*, **260**, 51.
- [21] WATANABE, J., KOMURA, H., and NIORI, T., 1993, *Liq. Cryst.*, **13**, 455.
- [22] WATANABE, J., HAYASHI, M., KINOSHITA, S., and NIORI, T., 1992, *Polym. J.*, **24**, 597.
- [23] DEL CAMPO, A., PÉREZ, E., and BELLO, A. (to be published).
- [24] LEVELUT, A. M., and TINH, N. H., 1987, *J. Phys.*, **48**, 847; JIN, J. I., and YUN, Y. K., 1995, *J. Phys. II Fr.*, **5**, 927.
- [25] ATTARD, G. S., GARNETT, S., HICKMAN, C., IMRIE, C. T., and TAYLOR, L., 1990, *Liq. Cryst.*, **7**, 495; ATTARD, G. S., DATE, R. W., IMRIE, C. T., LUCKHURST, G. R., ROSKILLY, S. J., SEDDON, J. M., and TAYLOR, L., 1994, *Liq. Cryst.*, **16**, 529.
- [26] TAKANISHI, Y., TAKEZOE, H., and FUKUDA, A., 1992, *Phys. Rev. B*, **45**, 7684.
- [27] IMRIE, C. T., and HENDERSON, P. A., 2002, *Curr. Opin. colloid interface Sci.*, **7**, 289.
- [28] WATANABE, J., NIORI, T., CHOI, S. W., TAKANISHI, Y., and TAKEZOE, H., 1998, *Jpn. J. appl. Phys.*, **37**, L401; WATANABE, J., NAKATA, Y., and SIMIZU, K., 1994, *J. Phys. II Fr.*, **4**, 581.